Facile partly templating growth of Bi_2S_3 nanorods by in-situ thermal sulphuration of BiOCl nanosheets and the photosensitive properties

Zhankui Cui ✉, *Erkang Hu, Hongtao Song*

Key Laboratory of Micro-Nano Materials for Energy Storage and Conversion of Henan Province, Institute of Surface Micro and Nano Materials, Xuchang University, Xuchang 461000, People's Republic of China
✉ *E-mail: zkcui@foxmail.com*

Published in Micro & Nano Letters; Received on 15th October 2017; Revised on 17th November 2017; Accepted on 15th December 2017

Bi_2S_3 nanorods were prepared by a facile in-situ thermal sulphuration method using BiOCl nanosheets as precursors. The products were characterised by X-ray diffraction, Raman scattering, Fourier-transform infrared spectroscopy and scanning electron microscopy. The optical properties were measured by ultraviolet-visible spectroscopy and photoluminescence techniques. The photosensitive properties were investigated by the photoelectrochemical method. The Bi_2S_3 sample was of pure orthorhombic phase and composed of nanorods with average diameter of ~200 nm and length of ~2 μm. A plausible gas phase growth mechanism was proposed which involved the partly templating of the shape of precursors by transforming BiOCl nanosheets to Bi_2S_3nanorods. The photocurrent of the products under irradiation of solar simulator reached 1.0 μA/cm^2 without bias voltage which was ten times that of the dark current. The photoelectric measurements clearly demonstrate that the as-prepared Bi_2S_3 nanorods possess excellent photosensitivity with stability and reproducibility, enabling the products suitable for the fabrication of high-performance photodetectors and other optoelectric devices.

1. Introduction: Bi_2S_3 belongs to an important category of $A_2^VB_3^{VI}$ (A = As, Sb, Bi; B = S, Se, Te) semiconductors and is composed of low-cost earth abundant non-toxic elements [1, 2]. Bi_2S_3 nanomaterials are in particular of interest due to their attractive thermoelectric, photoelectric and photocatalytic applications [3]. As one-dimensional nanomaterials can efficiently transport charge carriers while maintaining confinement across the diameter [4, 5], Bi_2S_3 nanorods exhibit significant capabilities acting as building blocks for advanced micro–nano devices such as photodetectors, chemical sensors, solar cells and supercapacitors [6–10].

Many approaches have been used to prepare Bi_2S_3 nanorods mainly including liquid phase methods. Xue *et al.* [11] prepared Bi_2S_3 nanorods through gelatin-assisted solution process under microwave irradiation; Helal *et al.* [12] synthesised Bi_2S_3 nanorods by hydrothermal method using $Bi(NO_3)_3{\cdot}5H_2O$ and thiourea as sources. Yu *et al.* [13] used colloidal chemistry method to produce Bi_2S_3 nanorods in the mixed solution of organic amines. Nevertheless, to the best of our knowledge, there are few reports on the preparation of Bi_2S_3 nanorods by gas phase method. The facile and low-cost fabrication routes of Bi_2S_3 nanorods are still needed to be developed.

Herein we report that Bi_2S_3 nanorods can be readily produced by an in-situ thermal sulphuration of BiOCl nanosheets in a vacuum tube furnace. The composition and morphology of the samples were characterised and the evolution mechanism of the gas phase synthetic process was investigated. The optical properties were examined including their light absorption properties and photoluminescence (PL) properties. A photodetecting device was constructed to evaluate the photosensitive properties of the as-prepared Bi_2S_3 nanorods by the photoelectrochemical method.

2. Experimental section: All the reagents are of analytical grade and were used without further purification. The precursing BiOCl nanosheets were prepared according to our previous report [14]. The synthesis of Bi_2S_3 nanorods was described as follows. Typically, 0.15 g BiOCl nanosheets and 0.15 g sulphur powder were put into a crucible and placed into the vacuum tube furnace, respectively. The temperature was elevated to 350°C at a rate of 5°C/min. The furnace was maintained at 350°C for 90 min. After that, it was allowed to cool to room temperature naturally and the products were collected for use.

X-ray diffraction (XRD) patterns were collected from a Bruker D8 Advance diffractometer with Cu Kα radiation at 1.54 Å. Raman spectrum was recorded on a Renishaw inVia spectrometer with a laser wavelength of 514 nm and Fourier-transform infrared (FTIR) spectrum was obtained from a Nicolet 6700 spectroscopy. The morphology observations were performed on a FEI Nova NanoSEM 450 microscopy. The optical properties were measured using a Cary 5000 UV–Vis-NIR spectroscopy and a Hitachi F-4600 fluorescence spectrophotometer (PL).

A photodetecting device was constructed to evaluate the photosensitive properties of the samples. Typically, a dimethylformamide dispersion of Bi_2S_3 nanorods was drop-cast on a 1 cm^2 Fluorine-doped Tin Oxide (SnO_2:F) (FTO) glass substrate and a Cu wire was connected to one of its edges using Ag slurry. The edges were sealed with epoxy resin to limit the direction of current during the photoelectrochemical test. A sun simulator (~100 mW/cm^2) was used as the light source. Current–time (*I–t*) and current–voltage (*C–V*) curves were recorded through a two-probe method on a CHI 660B electrochemical station. The electrolyte was composed of 0.5 M Na_2SO_4 solution and the counter electrode was a Pt coil.

3. Results and discussion: The crystal phases of the samples were characterised by XRD method. Fig. 1*a* shows the XRD patterns of BiOCl nanosheets and the samples sulphured for different times. As seen in the figure, the precursing BiOCl nanosheets were in accordance with JCPDS Card No. 850861. After thermal sulphuration for 1 min, there appeared new weak diffraction peaks at 28.6°, 25.1°, 32.0° and 22.4°, respectively. When the sulphuration time was 10 min, the diffraction intensity of above peaks became higher and more new diffraction peaks were present; almost all of the diffraction peaks of BiOCl phase remained at this stage. While for the sulphuration time of 90 min, all the diffraction peaks in the spectrum were assigned to the orthorhombic phase of Bi_2S_3 with JCPDS Card No. 751306, indicating the BiOCl precursors were completely transformed to Bi_2S_3 phase. Moreover, there were no intermediate phases formed in the sulphuration process, suggesting the purity of the Bi_2S_3 products.

The chemical composition and chemical bonds of the samples were studied by Raman and FTIR methods. Fig. 2*a* is the Raman spectrum of Bi_2S_3 nanorods. There were two obvious peaks present in the spectrum, locating at 119 and 960 cm^{-1}, respectively. The peak at 119 cm^{-1} was attributed to surface optical phonon modes which were caused by the effect of interface imperfections

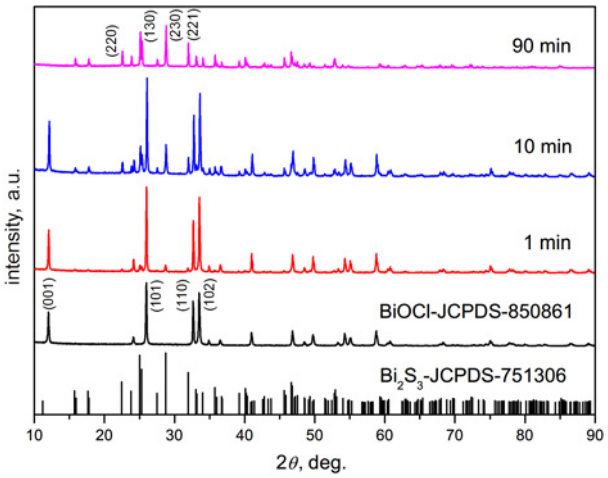

Fig. 1 *XRD patterns of BiOCl nanosheets and the samples sulphured for different times*

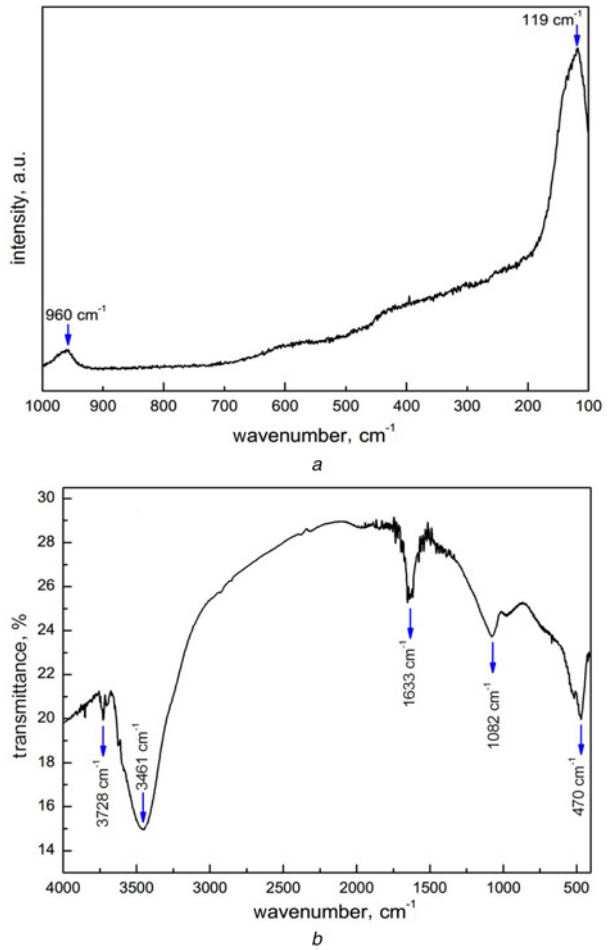

Fig. 2 *Raman spectrum and FTIR spectrum of Bi_2S_3 nanorods*
a Raman spectrum
b FTIR spectrum

of Bi_2S_3 nanostructures [15], while the peak at 960 cm^{-1} was assigned to Bi–S stretching vibrations [16]. The FTIR spectrum of Bi_2S_3 nanorods is displayed in Fig. 2*b*. There were five distinctive absorption bands in the spectrum, locating at 470, 1082, 1633, 3461 and 3728 cm^{-1}, respectively. The band at 470 cm^{-1} was attributed to Bi–S stretching vibrations and the band at 1082 cm^{-1} was corresponding to C–O stretching modes [17, 18]. The bands at 3461 and 1633 cm^{-1} were ascribed to the O–H stretching and bending modes of water; and the band at 3728 cm^{-1} could be assigned to dissociatively adsorbed water [19]. The Raman and FTIR results further confirm the formation of Bi_2S_3 phase during sulphuration process.

To reveal the formation of nanorods of Bi_2S_3 phase, scanning electron microscopy (SEM) technique was used. Fig. 3 displays the SEM images of BiOCl nanosheets and Bi_2S_3 nanorods. In Fig. 3*a*, BiOCl sample was composed of irregularly shaped nanosheets and the average size of BiOCl nanosheets is ~2 μm. The morphologies of the sulphured samples are shown in Figs. 3*b–d*. In Fig. 3*b*, there were some nanorods appearing on the surfaces of BiOCl nanosheets when the sulphuration time was 1 min. More nanorods were present and the BiOCl nanosheets disappeared gradually with prolonging the sulphuration time to 10 min, as shown in Fig. 2*c*. For the sulphuration time of 90 min, no BiOCl nanosheets were found shown in Fig. 2*d*, implying all of them were transformed to Bi_2S_3 nanorods and the average diameter of Bi_2S_3 nanorods is ~200 nm and the estimated average length is ~2 μm.

It is interesting to discuss the phase and morphology evolution mechanism of the thermal sulphuration process from BiOCl nanosheets to Bi_2S_3 nanorods. A plausible gas phase reaction related mechanism was proposed. The reaction equations are as follows and the mechanism illustration is represented in Fig. 4.

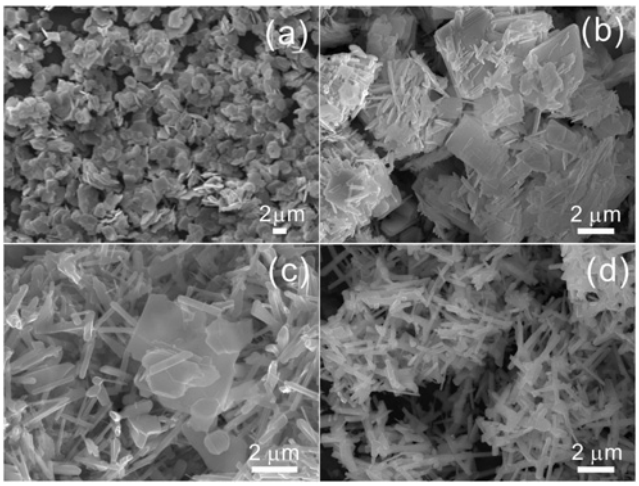

Fig. 3 *SEM images of*
a BiOCl nanosheets
b Samples sulphured for 1 min
c Samples sulphured for 10 min
d Samples sulphured for 90 min

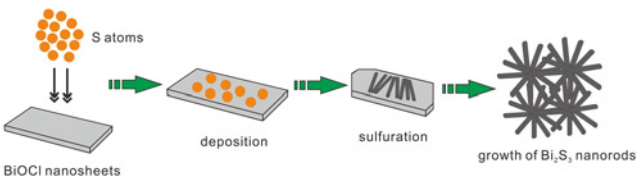

Fig. 4 *Illustration of the formation mechanism of Bi_2S_3 nanorods*

doi: 10.1049/mnl.2017.0744

When the sulphur powders were heated, they sublimed and some atoms from the sulphur gas were deposited on the surfaces of BiOCl nanosheets. The BiOCl nanosheets acted not only as catalysts for the formation of Bi_2S_3 nucleus but as templates for the further growth of Bi_2S_3 nanorods. The later sulphur atoms near the interfaces of Bi_2S_3 and BiOCl continued to react with BiOCl nanosheets, making the Bi_2S_3 nucleus grow along the surfaces of BiOCl nanosheets and form randomly distributed Bi_2S_3 nanorods. It was thought that the oriented growth of Bi_2S_3 nanorods was caused by that BiOCl nanosheets were partly templated by Bi_2S_3 phase, since when sphere Bi nanoparticles were used as bismuth source in the sulphuration process, sphere Bi_2S_3 nanoparticles were obtained but not Bi_2S_3 nanorods according to our previous report [20].

The photoelectric properties are closely related to the optical properties of the samples. The light harvesting and photoluminescent behaviours were measured by ultraviolet-visible (UV–Vis) spectroscopy and PL techniques, as shown in Fig. 5. Fig. 5*a* is the UV–Vis spectrum of Bi_2S_3 nanorods. As seen from the figure, the Bi_2S_3 nanorods exhibited excellent light absorption capacity in the visible light range. The corresponding light absorption edge was obtained from the perpendicular to the abscissa axis from the point of intersection of the two tangent lines from the absorption spectrum [21] and the value was 937 nm with the calculated optical bandgap of 1.32 eV which agreed well with the previous report [22]. Fig. 4*b* is the PL spectrum of Bi_2S_3 nanorods. When the sample was excited with light of 574 nm, an intense light emission occurred at 867 nm with the photon energy of 1.43 eV, which was also observed by Yu *et al.* [23]. Obviously, there was a blue shift of ~0.11 eV for PL compared with the measured bandgap of 1.32 eV. It could be explained by the quantum confinement effects induced by small sizes or band filling effects induced by surface defects [24].

To evaluate whether the as-prepared Bi_2S_3 nanorods could be used as photodetecting materials, the photoelectrochemical method was employed and the results are represented in Fig. 6. Fig. 6*a* is the current versus time (*I–t*) curve with zero bias voltage of Bi_2S_3 nanorods. In the figure, the dark current was 90 nA/cm^2 and the photocurrent reached 1.0 μA/cm^2. It clearly indicates that the photocurrent was approximately ten times that of dark current, suggesting the sample was very photosensitive. Moreover, the light-on photocurrent and the stable photocurrent after five cycles were retained at ~1.0 and 0.31 μA/cm^2, respectively, exhibiting the high stability and reproducibility of photosensitive properties. Fig. 6*b* is the current versus potential (*C–V*) curves of Bi_2S_3 nanorods. The dark current increased gradually with the elevated bias voltage varying from 90 nA/cm^2 to 2.2 μA/cm^2; while the photocurrent changed from 0.56 to 7.7 μA/cm^2 within the same bias voltage range. The inset of Fig. 6*b* shows the light-on photocurrent and the stable photocurrent became higher when increasing bias voltage, giving the value of 7.7 and 6.0 μA/cm^2 at the bias voltage of 0.6 V. The above results demonstrate that the as-prepared Bi_2S_3 nanorods are of highly photosensitive no matter with or without bias voltage.

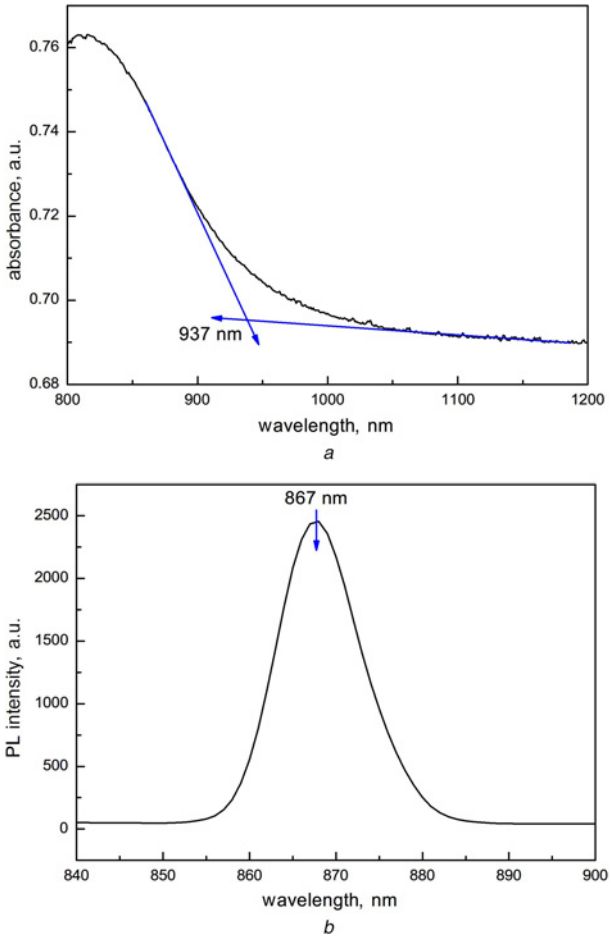

Fig. 5 *UV–Vis spectrum and PL spectrum of Bi_2S_3 nanorods*
a UV–Vis spectrum
b PL spectrum

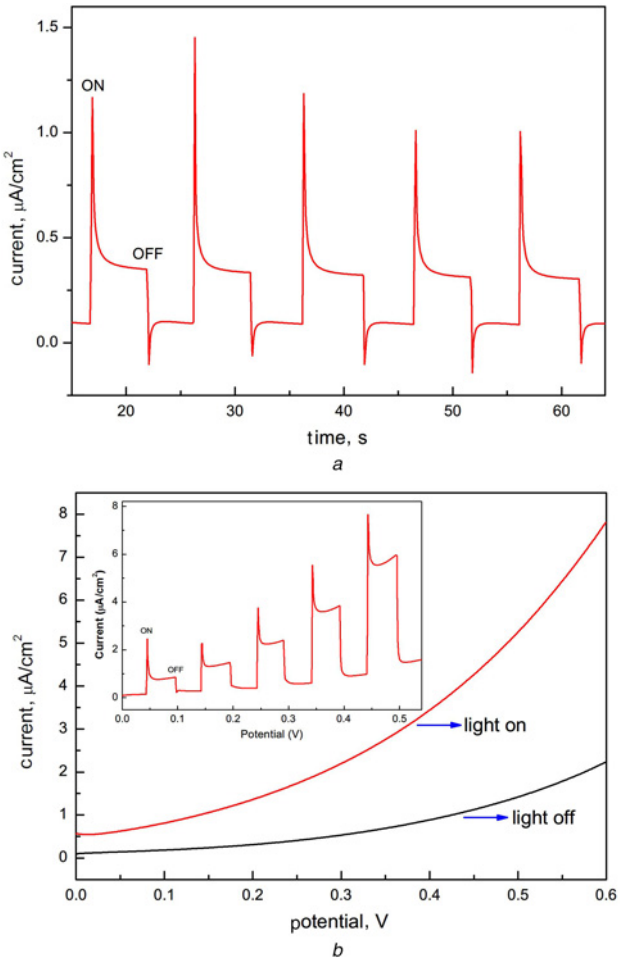

Fig. 6 *Current versus time curve and current versus potential curves when the light was on and off of Bi_2S_3 nanorods*
a Current versus time curve with zero bias voltage when the light was intermittently turned on and off of Bi_2S_3 nanorods
b Current versus potential curves when the light was on and off of Bi_2S_3 nanorods. Inset is current versus potential curve when the light was intermittently turned on and off of Bi_2S_3 nanorods

4. Conclusion: Bi_2S_3 nanorods were successfully prepared by a facile in-situ thermal sulphuration method using BiOCl nanosheets as precursors. The formation of Bi_2S_3 nanorods involved a gas phase reaction process during which the BiOCl nanosheets were partly templated by the oriented growth of Bi_2S_3 phase. The phase of Bi_2S_3 nanorods is pure and the mean diameter is ∼200 nm and the mean length is ∼2 μm. The light absorption edge is 937 nm and the PL peak is blue shifted to 867 nm. The photocurrent without bias voltage is 1.0 μA/cm^2 and the value reaches 7.7 μA/cm2 at the bias voltage of 0.6 V. Especially, the photocurrent without bias voltage is ten times that of the dark current. Our work reported here provides a facile and cost-efficient route for large-scale production of Bi_2S_3 nanorods which could be potentially used as highly photosensitive materials for the fabrication of photodetectors or other photoelectric devices.

5. Acknowledgments: The work was financially supported by the Science and Technology Bureau of Xuchang, the Basic and Frontier Technology Research Programs of the Department of Science and Technology of Henan Province (grant no. 162300410050), Natural Science Foundation of Xuchang University (grant no. 2016085).

6 References

[1] Dutta A.K., Maji S.K., Mitra K., *ET AL.*: 'Single source precursor approach to the synthesis of Bi_2S_3 nanoparticles: A new amperometric hydrogen peroxide biosensor', *Sens. Actuators B Chem.*, 2014, **192**, pp. 578–585

[2] Bernechea M., Cao Y., Konstantatos G.: 'Size and bandgap tunability in $B_{i2}S_3$ colloidal nanocrystals and its effect in solution processed solar cells', *J. Mater. Chem. A*, 2015, **3**, (41), pp. 20642–20648

[3] Ma J., Yang J., Jiao L., *ET AL.*: 'Bi_2s_3 nanomaterials: morphology manipulation and related properties', *Dalton. Trans.*, 2011, **40**, (39), pp. 10100–10108

[4] Chan C.K., Peng H., Twesten R.D., *ET AL.*: 'Fast, completely reversible Li insertion in vanadium pentoxide nanoribbons', *Nano Lett..*, 2007, **7**, (2), pp. 490–495

[5] Sun H., Deng J., Qiu L., *ET AL.*: 'Recent progress in solar cells based on one-dimensional nanomaterials', *Energy Environ. Sci.*, 2015, **8**, (4), pp. 1139–1159

[6] Ding T., Tian Y., Dai J., *ET AL.*: 'Building one-dimensional Bi_2S_3 nanorods as enhanced photoresponding materials for photodetectors', *Front. Optoelectron.*, 2015, **8**, (3), pp. 282–288

[7] Yang X., Tian S., Li R., *ET AL.*: 'Use of single-crystalline Bi_2S_3 nanowires as room temperature ethanol sensor synthesized by hydrothermal approach', *Sens. Actuators B Chem.*, 2017, **241**, pp. 210–216

[8] Liao H., Wu M., Jao M., *ET AL.*: 'Synthesis, optical and photovoltaic properties of bismuth sulfide nanorods', *CrystEngComm*, 2012, **14**, (10), pp. 3645–3652

[9] Yang H., Xie J., Li C.M.: 'Bi_2s_3 nanorods modified with $Co(OH)_2$ ultrathin nanosheets to significantly improve its pseudocapacitance for high specific capacitance', *RSC Adv.*, 2014, **4**, (89), pp. 48666–48670

[10] Tian Y., Ding T., Zhu X., *ET AL.*: 'Bi_2s_3 microflowers assembled from one-dimensional nanorods with a high photoresponse', *J. Mater. Sci.*, 2015, **50**, (16), pp. 5443–5449

[11] Xue B., Sun T., Mao F., *ET AL.*: 'Gelatin-assisted green synthesis of bismuth sulfide nanorods under microwave irradiation', *Mater. Lett.*, 2014, **122**, pp. 106–109

[12] Helal A., Harraz F.A., Ismail A.A., *ET AL.*: 'Controlled synthesis of bismuth sulfide nanorods by hydrothermal method and their photocatalytic activity', *Mater. Design*, 2016, **102**, pp. 202–212

[13] Yu H., Wang J., Wang T., *ET AL.*: 'Scalable colloidal synthesis of uniform Bi_2S_3 nanorods as sensitive materials for visible-light photodetectors', *CrystEngComm*, 2017, **19**, (4), pp. 727–733

[14] Cui Z.K., Hu E.K., Li S.L.: 'Modification of BiOCl nanosheets with Bi_2O_3 nanoparticles by a facile two step method and the enhanced photocatalytic performance of the composites', *J. Nano Res.*, 2017, **46**, pp. 203–211

[15] Xiao Y., Cao H., Liu K., *ET AL.*: 'The synthesis of superhydrophobic Bi_2S_3 complex nanostructures', *Nanotechnology*, 2010, **21**, (14), pp. 145601–145601

[16] Xu B., Wang G., Fu H.: 'Enhanced photoelectric conversion efficiency of dye-sensitized solar cells by the incorporation of flower-like Bi_2S_3: Eu^{3+} sub-microspheres', *Sci. Rep.*, 2016, **6**, pp. 233951–233959

[17] Kaur H., Singh B.: 'Direct electrochemical synthesis of bismuth (III) thiolates/dithiolates and their coordination compounds', *IOSR J. Appl. Chem.*, 2017, **10**, (6), pp. 32–35

[18] Wu J., Lan Z., Lin J., *ET AL.*: 'A novel thermosetting gel electrolyte for stable quasi-solid-state dye-sensitized solar cells', *Adv. Mater.*, 2007, **19**, (22), pp. 4006–4011

[19] Litke A., Su Y., Tranca I., *ET AL.*: 'Role of adsorbed water on charge carrier dynamics in photoexcited TiO_2', *J. Phys. Chem. C*, 2017, **121**, (13), pp. 7514–7524

[20] Cui Z., Li S., Zhou J., *ET AL.*: 'Preparation and optical properties of spherical Bi_2S_3 nanoparticles by in situ thermal sulfuration method', *NANO*, 2015, **10**, (2), pp. 15500211–15500216

[21] Luo X., Liu F., Li X., *ET AL.*: 'WO_3/TiO_2 nanocomposites: salt-ultrasonic assisted hydrothermal synthesis and enhanced photocatalytic activity', *Mater. Sci. Semicon. Process.*, 2013, **16**, (6), pp. 1613–1618

[22] Knapp C.E., Carmalt C.J.: 'Solution based CVD of main group materials', *Chem. Soc. Rev.*, 2016, **45**, (4), pp. 1036–1064

[23] Yu X., Cao C., Zhu H.: 'Synthesis and photoluminescence properties of Bi_2S_3 nanowires via surfactant micelle-template inducing reaction', *Solid State Commun..*, 2005, **134**, (4), pp. 239–243

[24] Yan Y., Liao Z., Bie Y., *ET AL.*: 'Luminescence blue-shift of CdSe nanowires beyond the quantum confinement regime', *Appl. Phys. Lett.*, 2011, **99**, (10), pp. 1031031–1031033

doi: 10.1049/mnl.2017.0744